Germline mutations in *BAP1* predispose to melanocytic tumors

Thomas Wiesner[1,2], Anna C Obenauf[3,4], Rajmohan Murali[2], Isabella Fried[1], Klaus G Griewank[2], Peter Ulz[3], Christian Windpassinger[3], Werner Wackernagel[5], Shea Loy[2], Ingrid Wolf[1], Agnes Viale[6], Alex E Lash[7], Mono Pirun[7], Nicholas D Socci[7], Arno Rütten[8], Gabriele Palmedo[8], David Abramson[9], Kenneth Offit[4,10], Arthur Ott[11], Jürgen C Becker[1], Lorenzo Cerroni[1], Heinz Kutzner[8], Boris C Bastian[2,12,13] & Michael R Speicher[3,13]

Common acquired melanocytic nevi are benign neoplasms that are composed of small, uniform melanocytes and are typically present as flat or slightly elevated pigmented lesions on the skin. We describe two families with a new autosomal dominant syndrome characterized by multiple, skin-colored, elevated melanocytic tumors. In contrast to common acquired nevi, the melanocytic neoplasms in affected family members ranged histopathologically from epithelioid nevi to atypical melanocytic proliferations that showed overlapping features with melanoma. Some affected individuals developed uveal or cutaneous melanomas. Segregating with this phenotype, we found inactivating germline mutations of *BAP1*, which encodes a ubiquitin carboxy-terminal hydrolase. The majority of melanocytic neoplasms lost the remaining wild-type allele of *BAP1* by various somatic alterations. In addition, we found *BAP1* mutations in a subset of sporadic melanocytic neoplasms showing histological similarities to the familial tumors. These findings suggest that loss of *BAP1* is associated with a clinically and morphologically distinct type of melanocytic neoplasm.

We report a type of melanocytic neoplasm that was inherited in an autosomal dominant pattern in two unrelated families and that was clinically, histopathologically and genetically distinct from common acquired nevi (**Fig. 1a**). Beginning in the second decade of life, affected family members progressively developed skin-colored to reddish-brown, dome-shaped to pedunculated, well-circumscribed papules with an average size of 5 mm (**Fig. 1b** and **Supplementary Figs. 1–4**). The number of tumors per individual varied markedly, ranging from 5 to over 50. No intellectual disabilities or dysmorphic features were identified in affected individuals.

Histopathological examination identified primarily dermal tumors composed entirely or predominantly of epithelioid melanocytes with abundant amphophilic cytoplasm and prominent nucleoli. The melanocytes often contained large, vesicular nuclei that varied substantially in size and shape (**Fig. 1c** and **Supplementary Figs. 5–7**). The cytological features of some of the cells were reminiscent of Spitz nevi; however, characteristic features (such as epidermal hyperplasia, hypergranulosis, Kamino bodies, clefting around junctional melanocytic nests and spindle-shaped melanocytes) frequently seen in Spitz nevi were consistently absent. In addition, 37 of 42 (88%) tumors in the families showed mutations in the *BRAF* proto-oncogene, which are typically absent in Spitz nevi[1].

Some of the neoplasms showed one or more atypical features such as high cellularity, considerable nuclear pleomorphism and several chromosomal aberrations. These tumors were classified as 'neoplasms of uncertain malignant potential', and the affected individuals were managed as if they had melanoma (**Supplementary Fig. 8**). Both families were identified because of the occurrence of multiple epithelioid melanocytic tumors, but, in each family, one affected individual had uveal melanoma, and three members of family 2 had been diagnosed with cutaneous melanoma (**Fig. 1a** and **Supplementary Table 1**).

We analyzed 22 melanocytic neoplasms from three affected individuals (II-1, II-4 and II-7) in family 1 by array-based comparative genomic hybridization (aCGH). We found losses affecting the entire chromosome 3 or portions of the short arm of chromosome 3 in 50% of tumors. The smallest overlap of the deleted regions encompassed 5.8 Mb, extending from position 47,976,758 to 53,848,761 (hg 18 assembly) and encoded at least 150 known genes (**Fig. 2a**).

The frequent loss of the 3p21 region suggested a second hit[2] resulting in the elimination of the remaining wild-type allele of a mutated tumor suppressor gene in this region. To support this hypothesis,

[1]Department of Dermatology, Medical University of Graz, Graz, Austria. [2]Human Oncology and Pathogenesis Program, Memorial Sloan-Kettering Cancer Center, New York, New York, USA. [3]Institute of Human Genetics, Medical University of Graz, Graz, Austria. [4]Cancer Biology and Genetics Program, Memorial Sloan-Kettering Cancer Center, New York, New York, USA. [5]Department of Ophthalmology, Medical University of Graz, Graz, Austria. [6]Genomics Core Laboratory, Memorial Sloan-Kettering Cancer Center, New York, New York, USA. [7]Computational Biology Center, Memorial Sloan-Kettering Cancer Center, New York, New York, USA. [8]Dermatopathologie, Friedrichshafen, Germany. [9]Department of Surgery, Memorial Sloan-Kettering Cancer Center, New York, New York, USA. [10]Clinical Genetics Service, Memorial Sloan-Kettering Cancer Center, New York, New York, USA. [11]Institute of Pathology, Medical University of Graz, Graz, Austria. [12]Department of Pathology, Memorial Sloan-Kettering Cancer Center, New York, New York, USA. [13]These authors contributed equally to this work. Correspondence should be addressed to T.W. (wiesnert@mskcc.org), B.C.B. (bastianb@mskcc.org) or M.R.S. (michael.speicher@medunigraz.at).

Received 16 February; accepted 22 July; published online 28 August 2011; doi:10.1038/ng.910

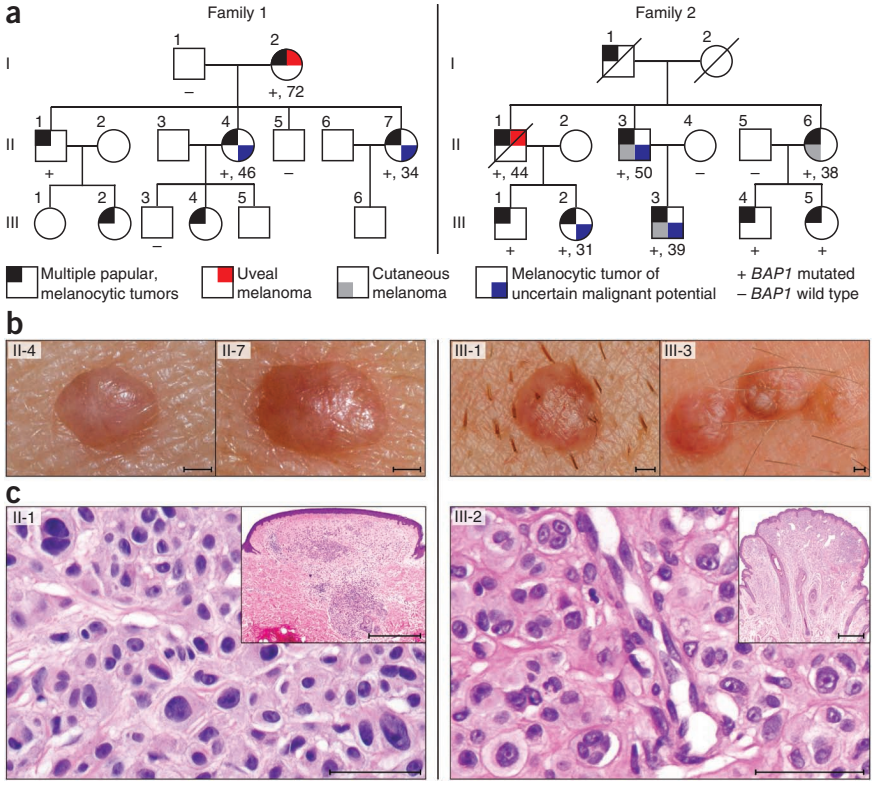

Figure 1 Pedigrees and clinical phenotypes of two affected families. Left panel shows family 1; right panel shows family 2. (**a**) Pedigrees. Ages of onset in years of the first melanoma or melanocytic tumor of uncertain malignant potential are written below the symbols. Only subjects older than 18 years were tested for mutations. An extended pedigree of family 1 is shown in **Supplementary Figure 15**. (**b**) Representative melanocytic neoplasms from affected individuals (II-4 and II-7 from family 1; III-1 and III-3 from family 2). Note the characteristic inconspicuous, skin-colored to reddish-brown, dome-shaped appearance. Scale bars, 1 mm. (**c**) Histopathology of representative melanocytic tumors from both families showing relatively symmetrical intradermal proliferations of large epithelioid melanocytes with abundant cytoplasm and enlarged, irregularly shaped vesicular nuclei, some with prominent nucleoli. Scale bars, 50 μm. Scale bars inset, 1 mm.

we reconstructed the haplotypes of six members of family 1 with SNP arrays. Affected siblings in the second generation (II-1, II-4 and II-7) inherited the same maternal copy of the 3p21 region, whereas the unaffected brother (II-5) received the other maternal 3p21 copy (**Supplementary Fig. 9a**). SNP arrays showed that, in all tumors with chromosome 3 loss, the paternal copy of chromosome 3 was lost, whereas the maternal copy was retained (**Supplementary Fig. 9b**). In conclusion, these data suggested that a mutated gene in the 3p21 region was inherited from the maternal side of the family.

To identify the mutated gene, we sequenced the minimally deleted region of chromosome 3 in two affected (I-2 and II-4) and two unaffected (I-1 and II-5) subjects from family 1 using an in-solution hybrid capture technique followed by massively parallel sequencing[3]. This analysis identified a frameshift mutation in *BAP1* (c.1305delG, p.Gln436Asnfs*135) that was subsequently found to segregate with the phenotype (**Fig. 2b** and **Supplementary Fig. 10**). To rule out *BAP1* germline mutations in the general population, we reviewed sequence data from 629 individuals in the 1000 Genomes Project database (see URLs). No truncating mutations were found, indicating that *BAP1* germline mutations are infrequent in the general population.

We assessed the status of the second *BAP1* allele in 29 skin tumors and in the uveal melanoma (I-2) from family 1 (**Supplementary Table 2**). All tumors in which loss of 3p21 was detected previously by aCGH also showed loss of the wild-type *BAP1* allele in the sequencing electropherogram (**Supplementary Fig. 11a**). In five additional cases without loss of the 3p21 region, the electropherogram showed markedly suppressed residual wild-type sequences, indicating that the neoplastic cells had lost the wild-type *BAP1* allele through copy-number–neutral mechanisms, resulting in maternal uniparental disomy (**Supplementary Fig. 11b**). In four other neoplasms without 3p21 deletions, we found additional acquired somatic nonsense (two cases), frameshift (one case) and missense (one case) mutations in *BAP1* (**Supplementary Fig. 11c**). Immunohistochemistry for BAP1 showed loss of nuclear expression in all melanocytic neoplasms, including the tumors without detectable alteration of the wild-type *BAP1* allele. In summary, these data suggest that the remaining wild-type allele of *BAP1* is lost by various somatic alterations in the melanocytic tumors.

In family 2, we found a different germline mutation in *BAP1* that segregated with the phenotype and removed the acceptor splice site at the last exon (c.2057-2A>G, p.Met687Glufs*28; **Fig. 2b**). Analysis of cDNA from two affected family members confirmed that the last intron was not removed by splicing (**Supplementary Fig. 12**). In family 2, inactivation of the remaining wild-type *BAP1* allele was found in 9 of 13 skin tumors, in the uveal melanoma (II-1) and in the cutaneous melanoma from individual II-3 (**Fig. 3a–d** and **Supplementary Table 3**). The metastatic melanoma of individual II-6 did not show loss of

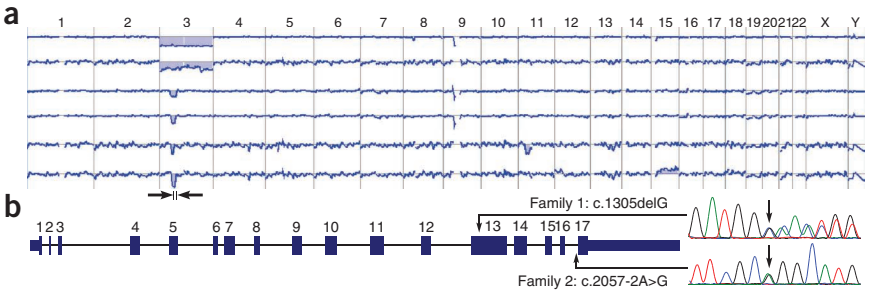

Figure 2 Identification of *BAP1* germline mutations. (**a**) aCGH profiles of recurrent deletions affecting chromosome 3 in the melanocytic neoplasms of family 1. The two top aCGH profiles illustrate deletions of the entire chromosome 3, whereas the other profiles show focal deletions in 3p21. The minimally deleted region (black arrows) encompassed approximately 6 Mb. The next to last profile shows an additional loss in chromosome 11 and the last profile a gain of chromosome 15. (**b**) Gene structure of *BAP1* and germline mutations observed in affected individuals from families 1 and 2.

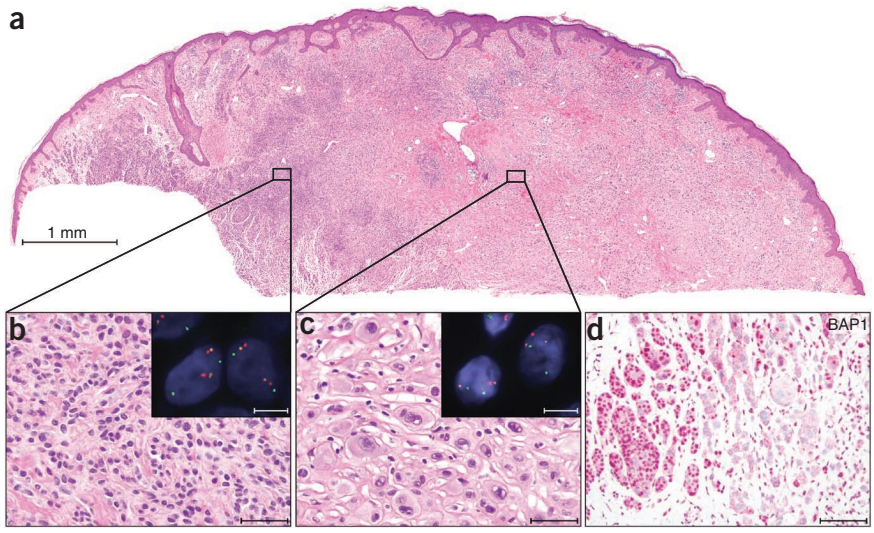

Figure 3 Biallelic *BAP1* loss is associated with characteristic histological features in familial melanocytic neoplasms. (**a**–**c**) A melanocytic neoplasm from individual III-3, family 2 (**a**), presents as a combined lesion with an area of small cells (common acquired nevus) on the left (**b**) and an area of large epithelioid cells on the right (**c**). Scale bars in **b**,**c**, 50 µm. Fluorescence *in situ* hybridization (red signal: 3p21 (*BAP1*); orange: 3p25 (control); green: 4p12 (control)) shows loss of *BAP1* in the area with large epithelioid melanocytes (inset in **c**: one red *BAP1* signal but two orange and green control signals per nucleus; scale bar, 10 µm) but no loss in the region of the common nevus (inset in **b**: two signals of each probe; scale bar, 10 µm). (**d**) BAP1 immunohistochemistry at the transition area between common nevus and epithelioid cell area showing a strong nuclear staining in the common nevus component (left) and loss of nuclear staining in the epithelioid component (right). Scale bar, 100 µm.

heterozygosity of *BAP1*, but no additional tissue was available to investigate alternative mechanisms of *BAP1* inactivation. Aside from the elevated, skin-colored melanocytic neoplasms, common acquired nevi (flat, brown maculae) were also excised from four subjects (II-3, III-3, III-4, III-5). Histopathologically, these nevi were composed of small uniform melanocytes and showed strong nuclear expression of BAP1 by immunohistochemistry (**Supplementary Fig. 13**).

To address the role of *BAP1* mutations in sporadic melanocytic neoplasms, we sequenced *BAP1* in 156 randomly selected tumors from patients without family history of melanocytic neoplasms: common nevi with uniform small melanocytes ($n = 28$); Spitz nevi ($n = 17$); neoplasms with overlapping features between Spitz nevus and melanoma (so-called 'atypical Spitz tumors', $n = 18$); primary melanomas originating from acral skin ($n = 15$), mucosa ($n = 15$) or skin with ($n = 15$) or without ($n = 15$) chronic sun-induced damage and uvea ($n = 33$). Thirteen (40%) uveal melanomas, two (11%) atypical Spitz tumors and three (5%) of the melanomas (two melanoma on skin without chronic sun-induced damage and one acral melanoma) had somatic *BAP1* mutations. No mutations were found in the other categories (**Supplementary Tables 4**–**8**). The mutation frequency seen in uveal melanoma is similar to that found in a recent report[4]. Two of five sporadic cutaneous melanomas that arose in nevi harbored *BAP1* mutations. In both cases, the *BAP1* mutations were absent in the nevus portion, suggesting that loss of function of *BAP1* may have a role in progression from nevus to melanoma in some cases (**Fig. 4a**–**g**).

The two atypical Spitz tumors with somatic *BAP1* mutations had similar morphologic features to the melanocytic neoplasms seen in both families, lacked immunohistochemical expression of BAP1 and harbored *BRAF* mutations (**Supplementary Fig. 14**). This finding suggests that biallelic inactivation of *BAP1* is associated with a clinically and morphologically distinct type of melanocytic neoplasm. Histopathologically, the tumors ranged from intradermal nevi composed of bland epithelioid melanocytes to atypical proliferations of epithelioid melanocytes with morphological and cytogenetic features overlapping with melanoma. Such tumors have been previously subsumed under the category of 'spitzoid' melanocytic neoplasms because they share cytological features with Spitz nevi.

As illustrated by these families, inheriting one mutant copy of *BAP1* results in a large number of these neoplasms. In aggregate, several hundred papular melanocytic tumors were present in affected family members, whereas the number of melanomas was substantially lower. This indicates that the risk of malignant progression in individual

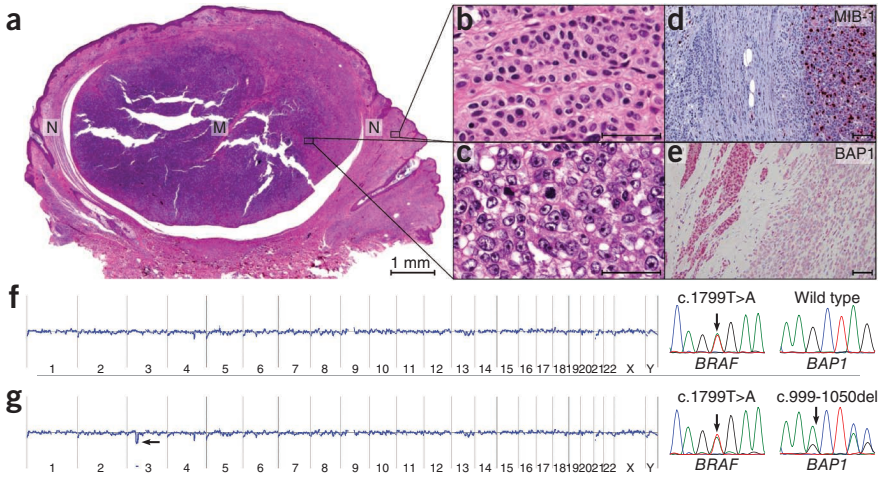

Figure 4 Progression of nevus to melanoma is associated with loss of *BAP1*. (**a**) Scanning magnification of a sporadic melanoma (M) arising within a nevus (N) (hematoxylin-eosin stain). (**b**) Nevus component with bland melanocytes containing monomorphous round and oval-shaped nuclei. Scale bar, 50 µm. (**c**) Melanoma component showing melanocytes with large vesicular nuclei and prominent nucleoli. Scale bar, 50 µm. (**d**) MIB-1 (Ki-67) immunohistochemistry showing a high proliferation rate in the melanoma compared to the nevus component. Scale bar, 100 µm. (**e**) BAP1 immunohistochemistry showing a conspicuous nuclear staining in the nevus contrasted with absent nuclear staining in the melanoma. Scale bar, 100 µm. (**f**) aCGH of the nevus component reveals no chromosomal aberrations. The electropherogram shows a *BRAF* p.Val600Glu mutation and no *BAP1* mutation. (**g**) aCGH of the melanoma component reveals a focal loss of chromosome region 3p21 spanning the *BAP1* locus. The electropherogram shows the same *BRAF* p.Val600Glu mutation and, in addition, a frameshift mutation of the second *BAP1* allele.

tumors is low and that biallelic loss of *BAP1* in conjunction with mutations in *BRAF* is not sufficient for melanoma formation in the skin. A recent report[4] proposed that biallelic loss of *BAP1* in uveal melanoma, which carry mutations in *GNAQ*[5] or *GNA11* (ref. 6) but not in *BRAF*, marks the transition to metastatic disease. Our findings may indicate that the role of *BAP1* in melanocytic neoplasia depends on the associated oncogene, the cell of origin or both.

BAP1 was originally discovered as a binding partner of BRCA1 and has been functionally implicated in DNA damage response[7,8], as well as in regulation of apoptosis, senescence and the cell cycle[9]. Its *Drosophila* counterpart Calypso is involved in chromatin remodeling, which was shown to oppose the monoubiquitination activity of polycomb repressive complex 1, a critical component of transcriptional silencing[10]. Mutations and deletions in *BAP1* have been reported in breast and lung cancers[11–13], but none of the individuals in our study developed breast or lung cancers.

In summary, we describe a new autosomal dominant syndrome that is caused by germline mutations of *BAP1*, characterized by a high penetrance of melanocytic neoplasms with distinctive clinical and histopathological features and possibly associated with an increased risk for uveal and cutaneous melanoma.

URLs. 1000 Genomes Project Database, http://www.1000genomes.org/; DNA-Chip Analyzer, http://biosun1.harvard.edu/complab/dchip/; Agilent's eArray, https://earray.chem.agilent.com/erray/; Genome Analysis Toolkit, http://www.broadinstitute.org/gsa/wiki/index.php/Local_realignment_around_indels; VarScan (v2.2), http://varscan.sourceforge.net/.

METHODS

Methods and any associated references are available in the online version of the paper at http://www.nature.com/naturegenetics/.

Accession numbers. The mutation nomenclature is based on the following National Center for Biotechnology Information (NCBI) reference sequences: *BAP1* cDNA, NM_004656.2; BAP1 protein, NP_004647.1; *BRAF* cDNA, NM_004333.4; BRAF protein, NP_004324.2; *GNAQ* cDNA, NM_002072.3; GNAQ protein, NP_002063.2; *GNA11* cDNA NM_002067.2; GNA11 protein, NP_002058.2.

Note: Supplementary information is available on the Nature Genetics website.

ACKNOWLEDGMENTS

We are indebted to all participating subjects for their enthusiastic participation in the study. We thank W. Stieber for clinical photography, U. Schmidbauer for providing histotechnical services, M. Leversha for performing FISH, A. Heguy for supporting sequencing, M. Asher for immunohistochemistry, H. Al-Ahmadie for assistance with the histological images and P. Dillinger for helping to collect the tissue samples. T.W. was supported by a Max-Kade Fellowship and expresses special thanks to H. Kerl for supporting, encouraging and inspiring his academic interests. A.C.O. is supported by the Austrian Science Fund (J3013) and K.G.G. by the Deutsche Forschungsgemeinschaft (GR 3671/1-1a). This work was funded by grants from the US National Institutes of Health (R01 CA131524), Geoffrey Beene Cancer Research Center (CC 66270), the American Skin Association (all to B.C.B.), the Andrew Sabin Family Foundation (to K.O.), the European Commission (GENINCA, contract no. HEALTH-F2-2008-202230) and the Jubilaeumsfonds of the Oesterreichische Nationalbank (13837).

AUTHOR CONTRIBUTIONS

Project planning and experimental design: T.W., B.C.B. and M.R.S. Review of clinical phenotypes: T.W., I.F., I.W. and J.C.B. Review of histology and immunohistology: T.W., B.C.B., H.K., R.M., L.C., I.F., A.R. and A.O. FISH analysis: T.W. and G.P. Sample collection: T.W., H.K., W.W., K.O. and D.A. aCGH: T.W. and A.C.O. Linkage analysis: A.C.O. and C.W. Mutation analysis: T.W., P.U. and S.L. Next-generation sequencing and data analysis: T.W., A.V., A.E.L., N.D.S. and M.P. Manuscript writing: T.W., B.C.B., R.M., M.R.S. and K.G.G. Revision of the manuscript: all authors.

COMPETING FINANCIAL INTERESTS

The authors declare no competing financial interests.

Published online at http://www.nature.com/naturegenetics/.
Reprints and permissions information is available online at http://www.nature.com/reprints/index.html.

1. Palmedo, G. *et al.* The T1796A mutation of the *BRAF* gene is absent in Spitz nevi. *J. Cutan. Pathol.* **31**, 266–270 (2004).
2. Knudson, A.G. Jr. Mutation and cancer: statistical study of retinoblastoma. *Proc. Natl. Acad. Sci. USA* **68**, 820–823 (1971).
3. Gnirke, A. *et al.* Solution hybrid selection with ultra-long oligonucleotides for massively parallel targeted sequencing. *Nat. Biotechnol.* **27**, 182–189 (2009).
4. Harbour, J.W. *et al.* Frequent mutation of *BAP1* in metastasizing uveal melanomas. *Science* **330**, 1410–1413 (2010).
5. Van Raamsdonk, C.D. *et al.* Frequent somatic mutations of *GNAQ* in uveal melanoma and blue naevi. *Nature* **457**, 599–602 (2009).
6. Van Raamsdonk, C.D. *et al.* Mutations in *GNA11* in uveal melanoma. *N. Engl. J. Med.* **363**, 2191–2199 (2010).
7. Matsuoka, S. *et al.* ATM and ATR substrate analysis reveals extensive protein networks responsive to DNA damage. *Science* **316**, 1160–1166 (2007).
8. Stokes, M.P. *et al.* Profiling of UV-induced ATM/ATR signaling pathways. *Proc. Natl. Acad. Sci. USA* **104**, 19855–19860 (2007).
9. Ventii, K.H. *et al.* BRCA1-associated protein-1 is a tumor suppressor that requires deubiquitinating activity and nuclear localization. *Cancer Res.* **68**, 6953–6962 (2008).
10. Scheuermann, J.C. *et al.* Histone H2A deubiquitinase activity of the Polycomb repressive complex PR-DUB. *Nature* **465**, 243–247 (2010).
11. Jensen, D.E. *et al.* BAP1: a novel ubiquitin hydrolase which binds to the BRCA1 RING finger and enhances BRCA1-mediated cell growth suppression. *Oncogene* **16**, 1097–1112 (1998).
12. Wood, L.D. *et al.* The genomic landscapes of human breast and colorectal cancers. *Science* **318**, 1108–1113 (2007).
13. Buchhagen, D.L., Qiu, L. & Etkind, P. Homozygous deletion, rearrangement and hypermethylation implicate chromosome region 3p14.3–3p21.3 in sporadic breast-cancer development. *Int. J. Cancer* **57**, 473–479 (1994).

ONLINE METHODS

Subjects. The study was approved by the Ethics Committees of the Medical University of Graz, Graz, Austria and Memorial Sloan-Kettering Cancer Center, New York, New York, USA and was conducted according to the Declaration of Helsinki. Written consent was obtained from all participating family members, and only subjects older than 18 years were included. Archival, paraffin-embedded tissue from both families, sporadic cutaneous and uveal melanomas, sporadic common melanocytic nevi, Spitz nevi and atypical Spitz tumors were retrieved from the Department of Dermatology, Medical University of Graz, Graz, Austria.

Family 1 was from southern Germany. We collected blood from seven individuals (I-1, I-2, II-1, II-4, II-5, II-7 and III-3), 29 melanocytic tumors from three affected subjects (II-1, II-4 and II-7) and one uveal melanoma from subject I-2 (**Fig. 1a** and **Supplementary Tables 1** and **2**). The melanocytic tumors of uncertain malignant potential of subject II-4 and II-7 were not available for molecular genetic analysis.

Family 2 was from southern Austria. We collected blood from nine individuals (II-3, II-4, II-5, II-6, III-1, III-2, III-3, III-4 and III-5), 11 melanocytic tumors from three affected subjects (II-3, III-2 and III-3), two melanocytic tumors of uncertain malignant potential from subjects II-3 and III-2, two cutaneous melanomas from subjects II-3 (nonmetastasizing melanoma) and II-6 (primary tumor and lymph node metastasis) and one uveal melanoma from subject II-1 (**Fig. 1a** and **Supplementary Tables 1** and **3**). The melanoma and the melanocytic tumor of uncertain malignant potential of subject III-3 were not available for molecular genetic analysis.

Histopathology and immunohistochemistry. Excised skin lesions were fixed in 4% neutral buffered formalin. The fixed tissues were processed according to routine histological methods and embedded in paraffin. Sections (5 µm thick) were cut from the paraffin blocks and stained with hematoxylin-eosin. Immunohistochemistry with an antibody against BAP1 (clone C4, Santa Cruz Biotechnology) was performed on tissue sections according to standard methods.

DNA extraction. Tumor-bearing tissue was manually microdissected from sections of archival paraffin-embedded samples of melanocytic tumors and melanomas. In the case of small tumors, tumor-bearing tissue was microdissected with a PALM Laser Microdissection and Pressure Catapulting system (Zeiss). DNA was extracted and purified from the microdissected tissue with the QIAamp DNA FFPE Tissue Kit (Qiagen) or the Chemagic DNA Tissue Kit (Chemagen) according to the manufacturer's instructions. DNA was also isolated from adjacent normal tissue to distinguish somatic from germline mutations.

Array-based comparative genomic hybridization. DNA samples were labeled using a Bioprime Array CGH Genomic Labeling Kit according to the manufacturer's instructions (Invitrogen). Briefly, 250–500 ng test and reference DNA samples (Promega) were differentially labeled with dCTP-Cy5 and dCTP-Cy3, respectively (GE Healthcare). Genome-wide analysis of DNA copy number changes was conducted using oligonucleotide arrays containing 60,000 or 180,000 probes according to the manufacturer's protocol version 6.0 (Agilent). Slides were scanned using Agilent's microarray scanner G2505B and analyzed with Agilent Feature Extraction and DNA Workbench software 5.0.14.

Sanger sequencing. The exonic regions of *BAP1* were divided into amplicons of 300 bp or less. Specific primers were designed with primer 3 and tagged with an M13 tail to facilitate Sanger sequencing (**Supplementary Table 9**). Primers for *GNAQ*, *GNA11* and *BRAF* were described previously[5,6,14]. The PCR reaction conditions were 0.25 mM dNTPs, 0.4× BSA (New England Biolabs), 1 U Hotstar Taq (Qiagen), 1× Hotstar Taq buffer (Qiagen) and 0.4 µM primer. PCR consisted of 35 cycles of 95 °C (45 s), 57 °C (45 s) and 72 °C (45 s) after initial denaturation at 95 °C for 5 min. PCR reaction products were purified with the QIAquick PCR Purification kit (Qiagen) and then used as templates for sequencing in both directions using Big Dye v3.1 (Applied Biosystems). Dye terminators were removed using the CleanSEQ kit (Agencourt Biosciences), and subsequent products were run on the ABI PRISM 3730xl (Applied Biosystems). Mutations were identified by using Sequencher software (Gene Codes) and only considered when variants were called in reads in both directions. All identified mutations were replicated at least twice. In sporadic tumors, germline DNA was sequenced from the adjacent normal tissue or blood to determine whether the mutations were somatically acquired.

RNA analysis. To evaluate the consequences of the splice-site germline mutation in family 2, we isolated RNA from whole blood of affected subjects and normal controls. The isolated RNA was reverse transcribed with Qiagen's Omniscript transcriptase and subsequently amplified with cDNA-specific primers for *BAP1* (**Supplementary Table 9**) employing the same PCR reaction described above. PCR products were electrophoretically separated on a 1% agarose gel. Bands were cut out, purified by gel purification (Promega Wizard SV-Gel and PCR cleanup system) and sequenced on a 3730xl capillary genetic analyzer (Applied Biosystems).

SNP arrays. DNA from four affected (I-2, II-1, II-4 and II-7) and two unaffected (I-1 and II-5) individuals from family 1 were analyzed with the Affymetrix GeneChip Mapping 500K array NspI chip. In accordance with the manufacturer's instructions, the arrays were scanned with a GeneChip Scanner, and the data were analyzed with GeneChip Operating Software (GCOS) and GeneChip Genotyping Analysis Software (GTYPE 3.0.2) to generate SNP allele calls. Haplotyping analysis was performed with the DNA-Chip Analyzer (see URLs) software under the assumption of an autosomal dominant trait.

Target enrichment and SOLiD sequencing. DNA capture was performed on 3 µg of high-quality genomic DNA using a custom SureSelect Target Enrichment kit according to the protocol provided by Agilent (Agilent). The baits library for SureSelect Target Enrichment was designed in Agilent's eArray (see URLs), contained 49,920 unique baits covering 3,291,328 bases, extended from base-pair position 47,501,754 to 54,373,721 according to hg18 assembly and will be provided upon request. 3p21-enriched DNA libraries of two affected (I-2 and II-4) and two unaffected subjects (I-1 and II-5) of family 1 were sequenced with SOLiD 4 according to the protocol provided by Applied Biosystems (Applied Biosystems), generating an average of 73,096,487 reads per samples with a read length of 50 bp. On average, 78% of the targeted region was covered at 400×.

To detect small insertion and deletion events, the SOLiD reads were mapped using the Burrows-Wheeler Aligner mapping program (v0.5.8c) with default options except for the colorspace switch. The mapped bam file was then processed to remove duplicated reads and realigned with the IndelRealigner from the Genome Analysis Toolkit (see URLs), which does a more careful alignment of reads around putative insertions and deletions. The realigned bam file was converted to a pileup with SAMtools and insertion/deletion variants were called with the VarScan (v2.2) program (see URLs).

Interphase fluorescence *in situ* hybridization. FISH probes were synthesized from BAC clones and labeled by nick translation with SpectrumGreen-dUTP, SpectrumRed-dUTP and SpectrumOrange-dUTP (Abbott) with standard procedures. The SpectrumRed probe mapped to 3p21 (RP11-447A21 and RP5-966M1), SpectrumOrange to 3p25 (RP11-614E19 and RP11-963B11RP) and SpectrumGreen to 4q12 (RP11-117E8 and RP11-231C18). The probes were hybridized on 5-µm–thick sections. The number of hybridization signals for these probes was assessed in a minimum of 200 interphase nuclei with strong and well-delineated contours.

Computational predictors of functional significance. The functional consequences of missense mutations in *BAP1* were assessed with three computational functional significance predictors (**Supplementary Tables 7** and **8**)[15–17].

14. Curtin, J.A. *et al.* Distinct sets of genetic alterations in melanoma. *N. Engl. J. Med.* **353**, 2135–2147 (2005).
15. Ng, P.C. & Henikoff, S. SIFT: Predicting amino acid changes that affect protein function. *Nucleic Acids Res.* **31**, 3812–3814 (2003).
16. Ramensky, V., Bork, P. & Sunyaev, S. Human non-synonymous SNPs: server and survey. *Nucleic Acids Res.* **30**, 3894–3900 (2002).
17. Reva, B., Antipin, Y. & Sander, C. Determinants of protein function revealed by combinatorial entropy optimization. *Genome Biol.* **8**, R232 (2007).

doi:10.1038/ng.910